

The Limitations of the WSR-88D Radar Network for Quantitative Precipitation Measurement over the Coastal Western United States



Kenneth J. Westrick,* Clifford F. Mass,* and Brian A. Colle[†]

ABSTRACT

An objective assessment of the WSR-88D radar coverage for detection and quantitative measurement of precipitation over the U.S. west coast is presented. As a result of significant terrain blockage, shallow precipitation, and low freezing levels, only one-fourth to one-third of the land surface in the region has sufficient radar coverage for precipitation estimation. Furthermore, it was found that the radar coverage is not representative of the precipitation distribution, with poor radar coverage in the regions where the most rainfall occurs.

Radar-derived storm-total precipitation estimates from the Portland, Oregon, radar for the catastrophic flood of February 1996 illustrate the limitations of the network, showing that the radar estimates in the heaviest precipitation regions to be less than 50% of the rain gauge values. A comparison of the WSR-88D coverage with the regional rain gauge network reveals that rain gauges will continue to be the major source of precipitation data over most of the region.

1. Introduction

In 1996, the last of the 136 operational Weather Surveillance Radar-1988 Doppler (WSR-88D) Next Generation Radar radar sites in the contiguous United States was put into operation, completing a major component of the National Weather Service (NWS) modernization program. This radar network, along with improvements in profilers and weather satellites, represents a continuing shift from in situ to remotely sensed measurements. The benefits of the WSR-88D in the western United States have been substantial, leading to improvements in short-range forecasts and contributing to a greater understanding of many regional weather phenomena (e.g., Colle and Mass 1998; Doyle 1997).

Most recent radar application research has evaluated the capabilities of the NWS network east of the Rocky Mountains, with a majority of these studies focusing on severe, convective-type events. As shown below, the often-encouraging results from these studies are not representative of radar capability over mountainous regions, especially for estimating quantitative precipitation.

The figure provided in Klazura and Imy (1993), a portion of which is shown in Fig. 1, is probably the most commonly cited estimate of radar coverage over the conterminous United States. In establishing the boundaries of radar coverage, Klazura and Imy (1993) determined the unblocked areas at 10 000 ft (3.05 km) above the radar sites; based on this criterion, there is radar coverage over a vast majority of the western United States. However, this approach produces an unrealistically optimistic estimate of useful radar coverage for quantitative precipitation measurement over the mountainous West. For example, previous studies of orographic precipitation (Houze et al. 1981; Marwitz 1983; Rauber 1992; Brintjes et al. 1994) show that much of the orographic precipitation enhancement occurs within a 1–2-km layer above terrain. Precipitation along the West Coast tends to be shallow and stratiform, and many western radar sites are

*Department of Atmospheric Sciences, University of Washington, Seattle, Washington.

[†]Institute for Terrestrial and Planetary Atmospheres, State University of New York at Stony Brook, Stony Brook, New York.

Corresponding author address: K. J. Westrick, Atmospheric Sciences, Box 351640, University of Washington, Seattle, WA 98195.

E-mail: westrick@atmos.washington.edu

In final form 28 May 1999.

©1999 American Meteorological Society

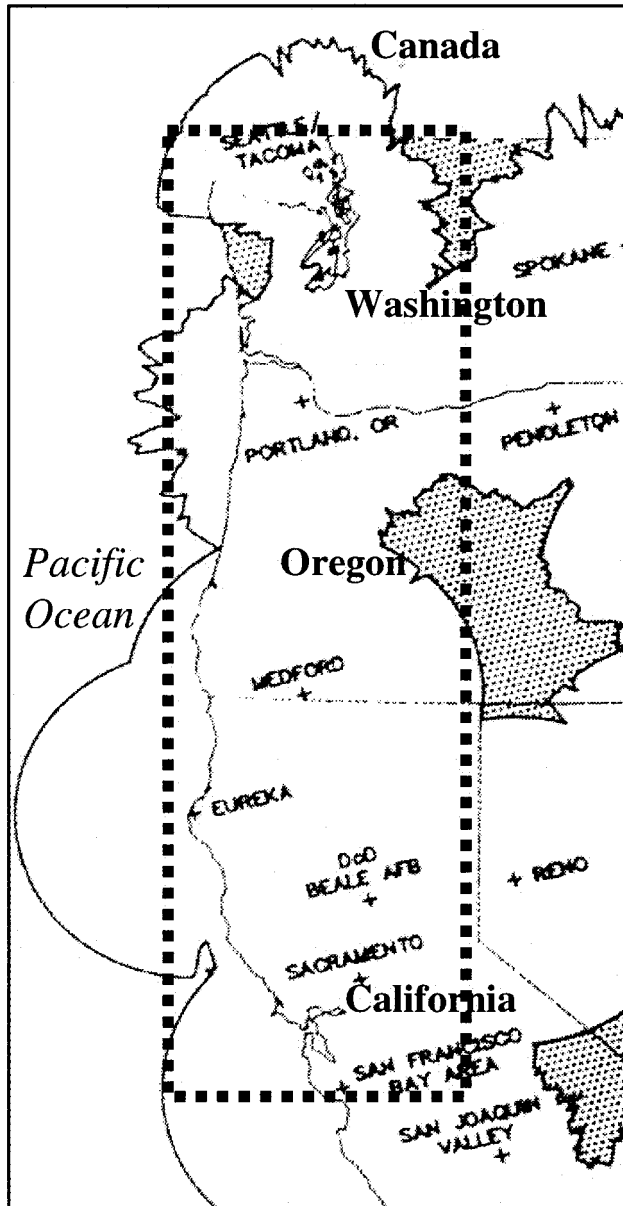


FIG. 1. WSR-88D network coverage at 10 000 ft (3.05 km) above the radar site for the western United States, adapted from Klazura and Imy (1993). Shaded regions denote land areas void of radar coverage, solid lines denotes the maximum radar coverage, and the dashed area encloses the region in this study.

at considerable elevation (e.g., Medford, 2300 m; San Francisco, 1077 m; Eureka, 760 m); a radar beam 3 km above these sites is often in the middle troposphere, most often far above the region of significant growth of hydrometeors.

In addition to the profound effects of shallow orographic precipitation and terrain blockage, western meteorological radars face the additional problem of a persistent wintertime “bright band” in the lower troposphere. With the relatively warm Pacific Ocean

upwind of the region, the relatively low melting level and the associated radar bright band make quantitative precipitation estimates based on reflectivity very difficult.

Although many West Coast meteorologists have come to the subjective realization that operational radar coverage is absent or marginal over most of the western United States, particularly over the higher terrain, only a handful of studies have examined this problem. Neyman (1996), in a comparison of WSR-88D precipitation with rain gauges over northwestern California, found that brightband contamination likely caused overestimation of precipitation in 12% of the samples, while beam blockage and beam overshooting of precipitation appeared to cause underestimation in 29% of the events. Reynolds (1995) suggested that a 0° elevation slice would be needed to significantly improve the precipitation estimates in shallow warm cloud systems sampled over the West Coast.

In response to the need for quantitative evaluation, this study provides an objective estimate of WSR-88D radar coverage along the west coast of the United States, a region where heavy precipitation and winter flooding represent the most significant damage-producing weather phenomena [NOAA’s *Storm Data*; NCDC (1959–93)]. In addition, we compare radar coverage with the distribution of rain gauges in order to evaluate their ability to extend and complement each other.

2. Evaluation of regional radar coverage

a. Methodology

This study evaluates radar coverage for the coastal zone of the western United States from roughly San Francisco to the Canadian border and from the eastern slopes of the Cascade/Sierra Mountains to the Pacific coast (Fig. 2). To determine the radar coverage for this region, topography from a 30 arc sec digital elevation dataset was interpolated to a 250-m horizontal resolution grid. Seven radar locations within the region (Table 1) were included in the analysis.¹ For each radar, the height of the top, center, and bottom of the 1° radar beam at each grid point was found using

¹The radars at Pendleton, OR; Reno, NV; and San Joaquin, CA, although outside the study region, were included in the analysis of radar beam height.

$$h = \left[r^2 + (k_e a)^2 + 2rk_e a \sin \theta_e \right]^{1/2} - k_e a,$$

where h is the height of the radar beam, r is the range from the nearest radar to the grid point, a is the radius of the earth, k_e is a constant $4/3$, and θ_e is the elevation angle (Doviak and Zrníc 1984). In the absence of strong inversions, Doviak and Zrníc state that the use of the constant k_e predicts beam height with sufficient accuracy for weather radar applications.

The first analysis estimated the range of the radar for precipitation detection. The height of the center of the radar beam above mean sea level and terrain level was determined for the region. If a particular radar beam was more than 50% blocked at a given range, the next higher beam was utilized for all regions beyond the blockage, assuming no more than 50% blocking occurred. If a beam was less than 50% blocked at all distances, the effective range of the radar was assumed to be 230-km horizontal distance, provided the center of the unblocked beam remained below 8 km. The maximum height of 8 km was selected based on research studies that show negligible radar returns at this level during stratiform precipitation events (Houze et al. 1981; Marwitz 1983; Rauber 1992).

The second set of analyses was designed to estimate the radar coverage for quantitative precipitation estimation. Consistent with the WSR-88D scan strategy (Fulton et al. 1998), the four lowest scan angles from the WSR-88D were considered.² Blockage was defined as the fraction of the beam blocked from the scan angle with the least fractional

blockage. As in the current WSR-88D algorithm, if the center of the beam from a particular tilt angle remains less than 50% terrain blocked, and the bottom of the beam clears the terrain by at least 150 m (O'Bannon 1997), the scan is used. If the blockage exceeds 50% for the center of a particular scan, the beam was considered not useful past that point, and the next higher scan was considered for ranges beyond. Also, if the center of the beam from a particular scan angle exceeded an upper elevation limit (discussed below), the

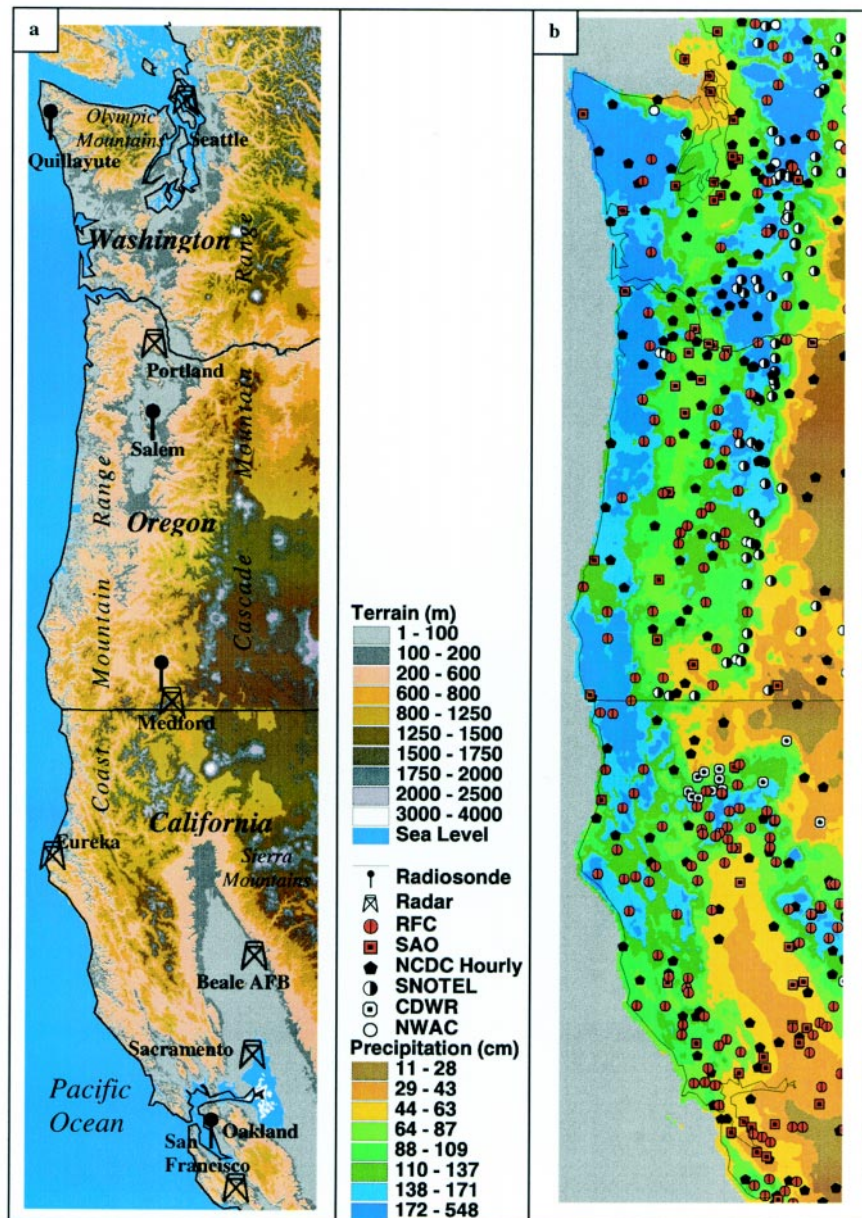


FIG. 2. (a) Coastal northwest U.S. topography and principal terrain features as well as upper-air and radar sites, and (b) rain gauge locations superposed over the PRISM-derived average annual precipitation.

²The 0.5°, 1.5°, 2.4°, and 3.4° scans were used.

TABLE 1. WSR-88D radar sites, their elevations (terrain elevation plus tower height), and effective ranges based on the average cool season melting level using the lowest (0.5°) radar scan and assuming no terrain blockage.

Radar	ID	Elev. of radar (m)	Effective range (km)
Camano Island–Seattle	KATX	181	92.0
Portland	KRTX	509	96.0
Medford	KMAX	2300	0.5
Eureka	KBHX	762	98.5
Beale AFB	KBBX	56	130.5
Sacramento	KDAX	39	131.0
San Francisco	KMUX	1077	82.5

beam was considered too high for surface precipitation rates to be determined.

Two methods were used to determine the upper elevation limit of the radar beam for effective radar coverage. The first method found the farthest distance in which the top of an unblocked scan³ remained within a 2-km layer above the local terrain. The 2-km above-ground-level estimate is based on studies that revealed sharp decreases in reflectivities at approximately this height above ground (Houze et al. 1981; Marwitz 1983; Rauber 1992; Collier 1993).

The second method assumes the maximum height of useful radar coverage is when the center of the beam intersects the lower edge of the melting/brightband level, which is assumed to be 300 m below the average freezing level. The use of the brightband level as an upper limit is based on the inability of the current WSR-88D Precipitation Processing System (PPS) to produce reliable quantitative surface rainfall estimates at or

above the melting level (Fulton et al. 1998).

The freezing levels used in the second method were based on a collection of heavy precipitation events at Oakland (CA), Medford (OR), Salem (OR), and Quillayute (WA) (Fig. 2a) that exceeded the thresholds shown in Table 2. Events were selected from a 34-yr record (1960–93) of 24-h precipitation totals, with the minimum precipitation threshold chosen so as to provide at least two heavy precipitation events per year at each location.⁴ Only precipitation events occurring from October through March were included in the analysis. The freezing levels associated with these heavy precipitation events were then averaged at each

location. As shown in Table 2, the average freezing level ranges from approximately 2.5 km at Oakland

⁴The average freezing level was found to be relatively insensitive to the number of heavy precipitation events considered. For example, when the minimum number of heavy precipitation events was increased from 66 to 198 (from an average of 2 to 6 heavy events per year), the average freezing level for each location changed by less than 10%.

TABLE 2. Total number of 24-h precipitation events included in the 34-yr period that met the minimum precipitation threshold, and the average, minimum, and maximum freezing levels observed during the events.

Observation location (and location of radar for which freezing level data applied)	24-h precipitation		Freezing level (meters MSL)		
	No. of events	Event threshold (cm)	Avg.	Max	Min
Oakland (applied to all CA radar)	77	9.6	2490	4390	830
Medford (Medford)	81	6.4	2110	3740	SFC
Salem (Portland)	74	9.6	2190	3900	190
Quillayute (Seattle)	151	12.8	1780	3780	SFC

³Less than 50% terrain blocked.

to less than 1.8 km at Quillayute. For all radar sites except Eureka, California, the closest upper-air-derived average freezing level (minus 300 m to allow for the melting of the precipitate) was used to compute the maximum range of the radar. Although Eureka is geographically closer to Medford, it is less likely to be influenced by cold continental air east of the Cascade Mountains, so it was felt that the higher freezing level determined at Oakland would provide a more representative freezing level for Eureka.⁵ The average effective ranges for quantitative precipitation estimation for the different radar locations using the average freezing level method are shown in Table 1.

b. Results

Figure 3a shows the height above mean sea level (MSL) for the lowest scan of the radar beams that are less than 50% blocked and below 8 km. This estimate of the maximum radar detection range for precipitation reveals data voids over the western slopes of the Olympics in Washington and over the Cascade ranges of central Oregon and northern Washington. Although this figure agrees reasonably well with Klazura and Imy (1993) (Fig. 1), it adds information about the *height* of the radar beam at different ranges from the radar. To highlight this elevation dependence, Fig. 3b shows the cumulative fraction of the land surface that has unblocked radar coverage⁶ at various elevations above ground or sea level. Although over 97% of the land surface is shown

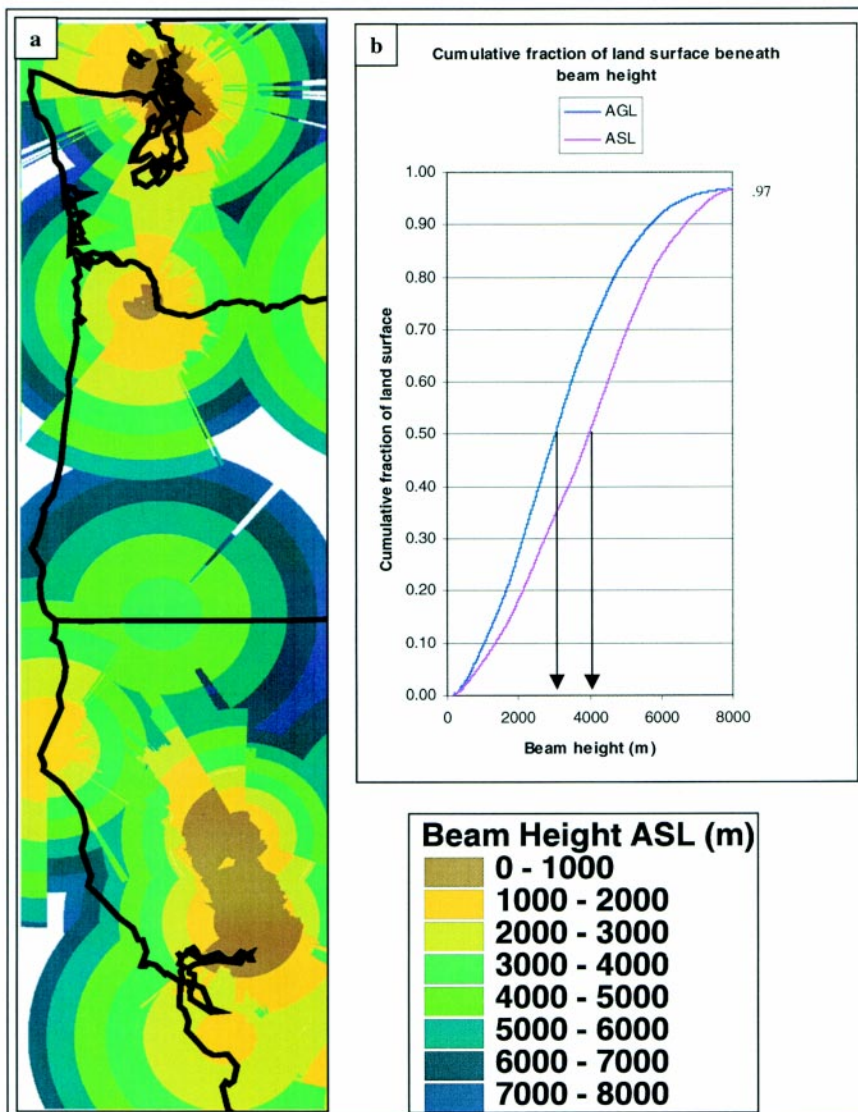


FIG. 3. (a) Height above mean sea level of the center of the radar beam (beams less than 50% terrain blocked), and (b) the corresponding cumulative fraction of the land surface with radar coverage at various heights above the ground (AGL) or sea level (MSL).

to have radar coverage below 8 km MSL, for a majority the radar beam is higher than 4 km MSL, or 3 km above ground level (AGL) (arrows in Fig. 3b).

The effective radar coverage for determining quantitative precipitation during the cool season using both the melting level and 2-km layer methods is shown in Fig. 4. Both methods produce very similar results. Even if the assumption is made that accurate quantitative precipitation estimation in partially radar blocked areas is possible, coverage is absent over two-thirds of the land portion of the coastal western United States. Less than one-quarter of the land surface has coverage if partially blocked regions are excluded. Blocking is nearly complete over most of the high ter-

⁵The extent of radar coverage over much of northern California may be optimistic as the freezing level is often 500 m lower over the west slopes of the Sierras than over Oakland during strong upslope flow and precipitation (Marwitz 1983).

⁶A beam is considered unblocked if it is less than 50% blocked.

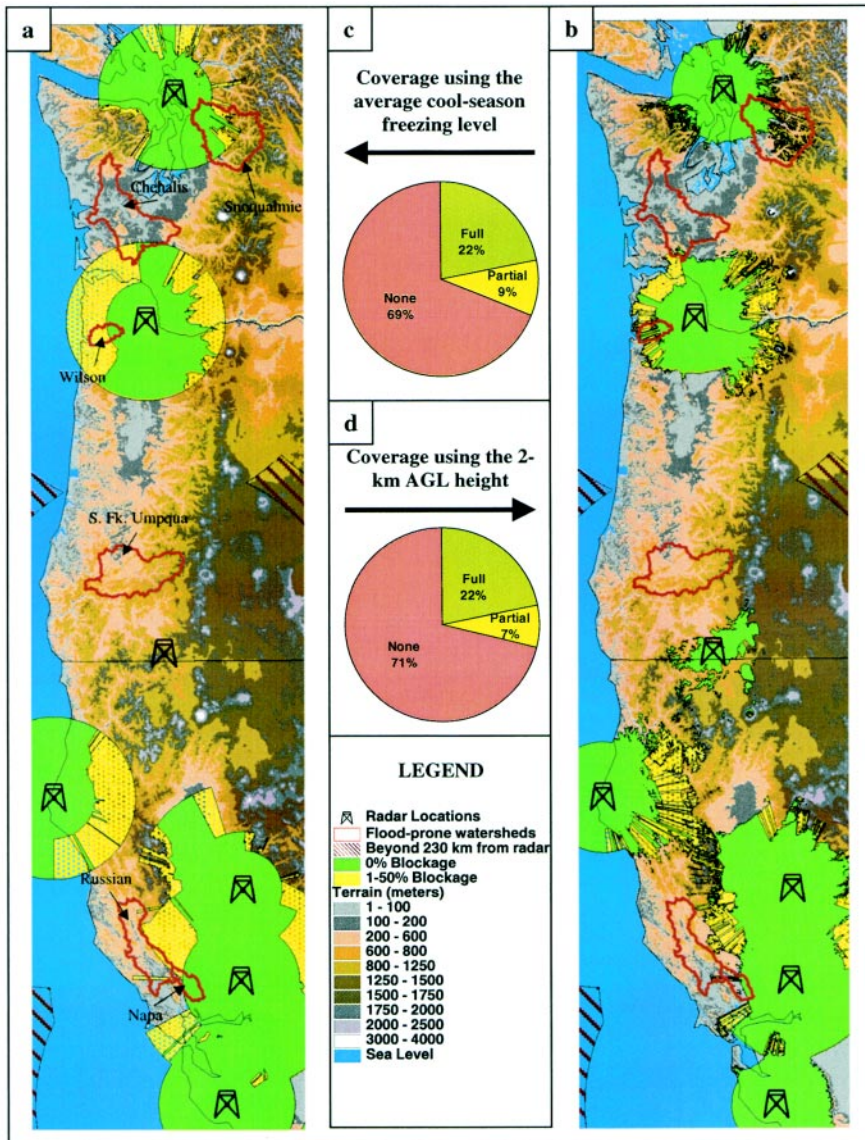


FIG. 4. Estimated WSR-88D radar coverage for the cool season over the coastal zone of the northwestern United States based on (a) the average freezing level and (b) 2 km AGL effective beam height. Six flood-prone watersheds are outlined in red, and regions 230 km beyond the nearest radar are shown with cross hatching. (c), (d) The percentage of land surface covered by radar is also shown.

rain of the coastal mountains and the Cascades, and coverage over the coastal ocean is essentially absent, except for the area west of Eureka. Figure 4 also indicates six flood-prone river basins that are of critical forecast concern [D. McDonnal, National Weather Service Forecast Office (NWSFO), Seattle, WA, 1999, personal communication; M. Van Tress, NWSFO, Portland, OR, 1999, personal communication; and an anonymous reviewer]. These include the Napa and Russian Rivers in California, the South Fork Umpqua and Wilson Rivers in Oregon, and the Chehalis and

Snoqualmie Rivers in Washington. Coverage over these watersheds is either extremely poor or nonexistent. It is also worth noting that with the melting-level method there is virtually no useful quantitative precipitation information from the Medford radar.

A major failing of the present radar coverage is that it does not provide a spatially representative sampling of the regional precipitation distribution. Comparing the 1960–91 precipitation climatology derived by the Parameter-elevation Regressions on Independent Slopes Model (PRISM) program (Daly et al. 1994) (Fig. 2b) with the radar coverage shown in Fig. 4a, reveals that there is little radar coverage over the regions of heaviest climatological precipitation, with the coastal lowlands being the only regions fairly well covered by radar.

A recent major flood event underscores the radar coverage problem in the region. During the winter of 1995/96, exceptionally heavy seasonal precipitation (125%–175% of the mean) occurred over the Pacific Northwest (Halpert and Bell 1997; Colle and Mass 1999). The most significant event of this period took place on 5–9 February 1996, when many rivers in northwest Oregon and

southwest Washington experienced the worst flooding in 30 years. The Columbia and Willamette Rivers rose to as much as 20 ft above flood stage, over 30 000 residents were forced from their homes, and eight deaths and nearly \$500 million of damage were directly attributed to the floods (NCDC 1996). This event provides a good test of the precipitation coverage and quantitative precipitation products from the Portland WSR-88D radar.

Using over 130 National Weather Service (Surface Aviation Observation, SAO), National Climatic Data

Center (NCDC) cooperative observer program (COOP), and Snow-Telemetering (SNOTEL) rain gauge stations, a storm-total precipitation map was constructed for southwestern Washington and northwestern Oregon for the 5–9 February 1996 event. Isohyets derived from the rain gauge observations were superposed on the storm-total map produced by the Portland (RTX) WSR-88D standard quantitative precipitation algorithm (Fig. 5). The heaviest precipitation, exceeding 500 mm of liquid-equivalent precipitation, fell over the coastal range of northwestern Oregon and the southwestern Washington Cascades, while over the lowlands, such as the Willamette Valley of northern Oregon, around 200 mm of precipitation was observed. The freezing level varied between 1.5 and 2.7 km MSL during this 4-day event.

Many problems are evident in the radar-derived precipitation. For example, partial or complete terrain blockage degraded quantitative precipitation estimation where the heaviest precipitation fell, such as over the lower windward slopes of the Cascades. The radar-derived precipitation underestimated the rain gauge measurements by 30%–40% over the Oregon coastal range, where 400–500 mm of precipitation fell. There is also considerable underestimation in the radar-derived storm totals over many regions considered to be partially obscured (Fig. 3), such as immediately to the west and northwest of the radar. There are noticeable circular bands at various distances away from the radar in the storm-total precipitation, which likely resulted from various radar scans (0.5°, 1.5°, and 2.6° elevations) intersecting the melting level aloft. Serendipitously, the estimated precipitation within some of these artificial bands is close to observed (around 200 mm) for some lowland areas; however, because of the limited number of radar scans at low levels there are gaps between the bands in which the precipitation is dramatically underestimated. It is also worth noting the extremely low or zero values of precipitation over the Chehalis River region in Washington (for location see Fig. 4a), even though the flood of record occurred at this time (D. McDonnal 1999, personal communication). Clearly, the Portland WSR-88D had limited useful-

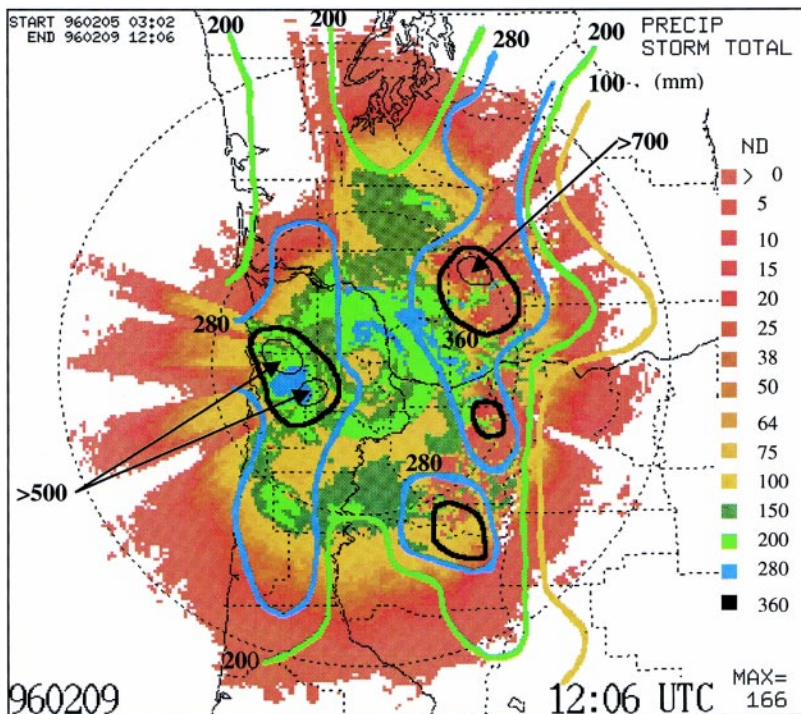


FIG. 5. Storm-total precipitation for the period 0300 UTC 5 Feb–1200 UTC 9 Feb 1996 from the WSR-88D radar at RTX. Also plotted are the observed isohyets produced from data taken from over 130 rain gauges.

ness in determining the magnitude and distribution of precipitation during this event, especially in the regions of heaviest precipitation.

3. The regional rain gauge network and its relationship to radar coverage

Using the PRISM climatological precipitation fields as ground truth, the availability of rain gauge data as a function of annual precipitation and radar coverage was analyzed (Figs. 2b and 6). It is apparent from Fig. 2b that the real-time SAO network does not uniformly capture the precipitation distribution, with relatively few sites in the mountainous regions, where the heaviest precipitation is observed, and in the arid regions, with annual precipitation less than 28 cm (Fig. 2b). The inclusion of the RFC⁷ gauges significantly improves the coverage, especially in areas of moderate annual precipitation (29–87 cm), such as the Puget

⁷RFC denotes a variety of precipitation gauge sites, available in real time, compiled by the regional River Forecast Centers (RFC), and forwarded to the National Centers for Environmental Prediction daily.

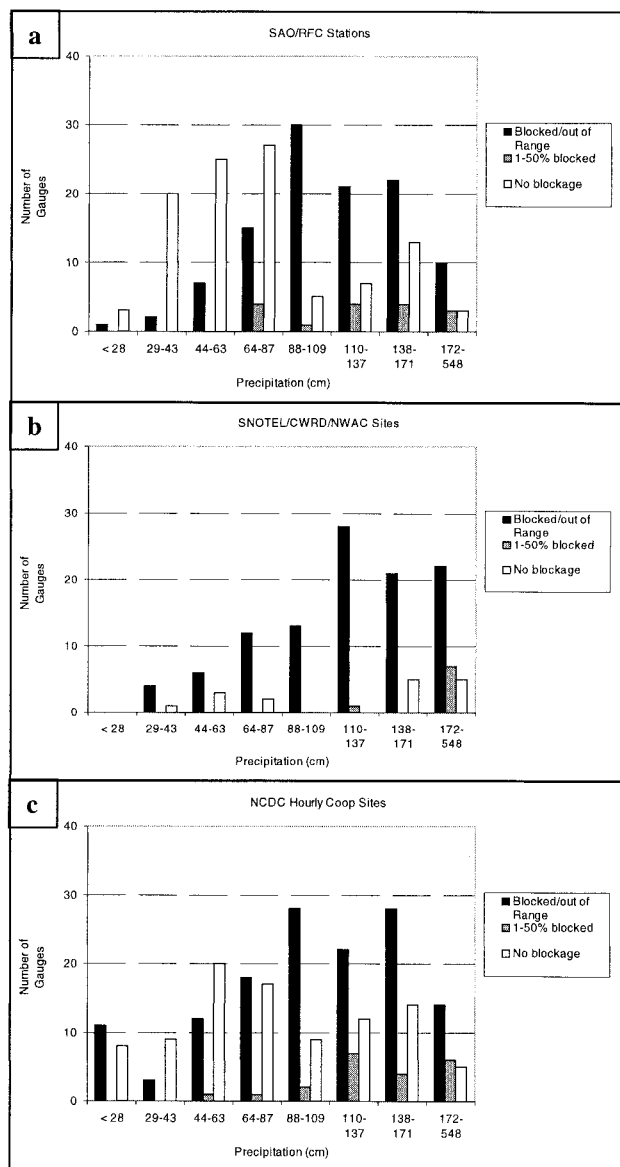


FIG. 6. The number of rain gauges by mean annual precipitation and radar coverage based on average freezing level. Included in the breakdown are (a) Surface Aviation Observations (59 sites) and gauges (169 sites) included in the Northwest and California-Nevada River Forecast Center's "precipitation update" product; (b) National Resources Conservation Service SNOTEL (83 sites), California Division of Water Resources (28 sites), and Northwest Avalanche Center (19 sites); and (c) National Climate Data Center hourly (251 sites).

Sound lowlands and the Willamette and San Joaquin Valleys (Fig. 2b). A relatively high percentage of the SAO/RFC sites are located in regions of partial or complete radar coverage (Fig. 6a; Table 3), suggesting their potential value for enhancing radar-derived precipitation estimates in those areas.

Real-time precipitation observations are also available from the SNOTEL network (Shafer and Burke

1979), maintained by the National Resource Conservation Services and a number of regional cosponsoring agencies, and networks run by the California Division of Water Resources (DWR) and the Northwest Avalanche Center (NWAC). As shown in Figs. 2b and 6b, these sites are generally in regions of higher terrain and greater precipitation, where radar blockage problems are most acute (Table 3). Thus, they are important complements to both the SAO/RFC and radar networks, and have proven invaluable for model precipitation verification over West Coast terrain (Colle et al. 1999). A shortcoming of the SNOTEL network is its coarse precipitation recording resolution (2.54 mm) and its reporting of data at local standard time rather than UTC, complicating model verification. Many of the high terrain stations rain gauges also suffer from precipitation undercatchment, a problem that is considerably worse during windy conditions with frozen precipitate (Larson and Peck 1974; Yang et al. 1998), underscoring the necessity for anemometers at these sites. Fortunately, the SNOTEL and DWR sites have snow pillows, which do not suffer from undercatchment, thus providing an independent method for determining precipitation estimates during frozen precipitation events. In addition, all of these sites are telemetered and available in near-real time; this is of utmost importance to forecasters.

The NCDC hourly precipitation sites (Fig. 2b) form the most spatially representative network (cf. pie charts in Fig. 4 with Table 3), providing the best sampling over the drier portions of the region, as well as areas of heavier precipitation (Fig. 6c). Unfortunately, most of these sites are not equipped with wind shields, creating the potential for significant undercatchment, and the recording resolution for the majority of the gauges is the relatively coarse 2.54 mm. Furthermore, since most of the NCDC sites are not telemetered, the data are not available for several months after collection.

4. Summary and conclusions

An assessment of the WSR-88D network's coverage for both detection and quantitative measurement of precipitation over the west coast of the United States reveals significant gaps. Although approximately 97% of the land surface area could be considered to be radar covered for precipitation detection, for at least 50% of the land region the radar beam is more than 4 km above sea level and 3 km above ground.

For accurate quantitative precipitation measurement by radar during the cool season, when a vast majority of the heavy precipitation events occur, over two-thirds of the land surface of the region is void of radar coverage. This assumes that accurate quantitative precipitation estimates are possible in partially blocked regions. Less than one-quarter of the land region is covered if partially blocked regions are excluded. These assessments are based on the assumption that the average cool season melting level serves as the maximum effective height of the radar beam for quantitative precipitation assessment. Blocking is nearly complete over most of the high terrain of the coastal mountains and Cascades, and coverage over the coastal ocean is essentially absent, except for the area west of Eureka. A second method that determined the farthest distance in which the top of a radar scan remained within a 2-km layer above the local terrain produced virtually identical results.

It is shown that radar-derived areal precipitation estimates are not representative of the regional precipitation climatology, since radar coverage is limited to lowland areas of moderate precipitation, and are nearly absent for regions of high terrain and precipitation. An analysis of the catastrophic flood of 5–9 February 1996 highlights the inability of one radar (Portland) to properly define heavy precipitation occurring over the Cascades and the coastal mountains.

Although improvements to the WSR-88D PPS have undoubtedly improved radar-derived quantitative estimates near the radar site, the extensive blocking and brightband effects endemic to the region will continue to considerably limit the extent and usefulness of radar-based precipitation measurements. Currently the radar is restricted from going below 0.5° elevation, but a possible method of increasing the regional radar coverage would be the implementation of 0° and/or negative scan angles. This would be particularly advantageous for those western radars located at high elevation. For example, the effective areal coverage at the 3-km AGL level for the Medford radar would increase by nearly a factor of 3 if a 0° scanning angle were used. Additional scans at the

TABLE 3. Quantity and percentage of rain gauges broken down by radar coverage based on the average cool season (Oct–Mar) freezing level effective beam height.

	SAO/RFC		SNOTEL/DWR/ NWAC		NCDC hourly COOP	
	Quantity	Percent	Quantity	Percent	Quantity	Percent
Zero blockage	101	44	16	11	92	37
1%–50% blockage	18	8	8	6	20	8
> 50% blockage or lowest unobstructed beam > average freezing level	108	48	107	83	139	55

shallower angles may also mitigate the continuity problems evident in the radar-derived spatial precipitation fields (Fig. 5). In addition to improvements in the preexisting radar network, more radar sites must be added over the western United States, particularly near the coastline, where terrain blockage is less of a problem. The Pacific Northwest, a region with a large fishing industry, major international seaports, and large navy facilities, has virtually no meteorological radar coverage over the coastal waters, in stark contrast to the rest of the nation.

But even if all the above improvements and additions to the western radar network are realized, the regional rain gauge network will continue to be the principal instrument for determining the extent and quantity of precipitation throughout a significant portion of the western United States, particularly over mountainous regions. With that reality in mind, continued emphasis on the precipitation gauge network is required. Increasing the density of *reliable* rain gauges in the radar-coverage-void regions would certainly be a major contribution toward the effort, although a sound plan needs to be developed for locating the sites. An effort to telemeter the existing gauges, especially in radar-coverage-void regions, is required so that precipitation data are available for forecasters in real time. In addition, research aimed at integrating the existing radar data with that available from the rain gauge network, especially at the “overlap” region where radar coverage diminishes, is needed. Only by adopting such a two-pronged approach, using both remote sensing and in situ measurements, will significant progress toward defining the actual distribution

of precipitation over the coastal western United States be made.

Acknowledgments. This research was supported by a COMET fellowship grant (UCAR 597-86990) as well as support from the ONR Coastal Meteorology Accelerated Research Initiative (Grant NH45543-4454-44) and the National Science Foundation (ATM-9634191). The authors wish to thank three anonymous reviewers for extremely insightful and helpful comments that contributed to many improvements in this paper. The authors also thank Dr. Sandra Yuter and Curtis James at the University of Washington for reading the original manuscript and providing helpful comments and contributions. Information pertaining to the River Forecast Center precipitation update product was provided by Don Laurine of the Pacific Northwest River Forecast Center and Eric Strem of the California–Nevada River Forecast Center.

References

- Bruintjes, R. T., T. L. Clark, and W. D. Hall, 1994: Interaction between topographic airflow and cloud precipitation development during passage of a winter storm in Arizona. *J. Atmos. Sci.*, **51**, 48–67.
- Colle, B. A., and C. F. Mass, 1998: Windstorms along the western side of the Washington Cascade Mountains. Part I: A high-resolution observational and modeling study of the 12 February 1995 event. *Mon. Wea. Rev.*, **126**, 28–51.
- , and —, 1999: The 5–9 February 1996 flooding event over the Pacific Northwest: Sensitivity studies and evaluation of the MM5 precipitation forecasts. *Mon. Wea. Rev.*, in press.
- , K. J. Westrick, and C. F. Mass, 1999: Evaluation of MM5 and Eta-10 precipitation forecasts over the Pacific Northwest during the cool season. *Wea. Forecasting*, **14**, 137–154.
- Collier, C. G., 1993: The measurement of rainfall. *Land Surface Processes in Hydrology—Trials and Tribulations of Modeling and Measuring*, S. Sorooshian, G. V. Hoshin, and J. C. Rodda, Eds., Springer, 75–111.
- Daly, C., R. P. Neilson, and D. L. Phillips, 1994: A statistical–topographic model for mapping climatological precipitation over mountainous terrain. *J. Appl. Meteor.*, **33**, 140–158.
- Doviak, R. J., and D. S. Zrnic, 1984: *Doppler Radar and Weather Observations*. Academic Press, 593 pp.
- Doyle, J. D., 1997: The influence of mesoscale orography on a coastal jet and rainband. *Mon. Wea. Rev.*, **125**, 1465–1488.
- Fulton, R. A., J. P. Breidenbach, D. J. Seo, and D. A. Miller, 1998: The WSR-88D rainfall algorithm. *Wea. Forecasting*, **13**, 377–395.
- Halpert, M. S., and G. D. Bell, 1997: Climate assessment for 1996. *Bull. Amer. Meteor. Soc.*, **78**, S1–S49.
- Houze, R. A., S. A. Rutledge, T. J. Matejka, and P. V. Hobbs, 1981: The mesoscale and microscale structure and organization of clouds and precipitation in midlatitude cyclones. III: Air motions and precipitation growth in a warm-frontal rainband. *J. Atmos. Sci.*, **38**, 639–649.
- Klazura, G. E., and D. A. Imy, 1993: A description of the initial set of analysis products available from the NEXTRAD WSR-88D system. *Bull. Amer. Meteor. Soc.*, **74**, 1293–1311.
- Larson, L. L., and E. L. Peck, 1974: Accuracy of precipitation measurements for hydrologic modeling. *Water Resour. Res.*, **10**, 857–863.
- Marwitz, J. D., 1983: The kinematics of orographic airflow during Sierra storms. *J. Atmos. Sci.*, **40**, 1218–1227.
- NCDC, 1959–93: *Storm Data*. Vols. 1–35.
- , 1996: *Storm Data*. February.
- Neyman, L. M., 1996: Initial comparison of WSR-88D precipitation products and rain gauge precipitation for northwestern California. Western Region Tech. Attachment 96–21, 5 pp. [Available from NWS Western Region Headquarters, Federal Building, Salt Lake City, UT 84138.]
- O’Bannon, T., 1997: Using a ‘terrain-based’ hybrid scan to improve WSR-88D precipitation estimates. Preprints, *28th Conf. on Radar Meteorology*, Austin, TX, Amer. Meteor. Soc., 506–507.
- Rauber, R. R., 1992: Microphysical structure and evolution of a central Sierra Nevada orographic cloud system. *J. Appl. Meteor.*, **31**, 3–24.
- Reynolds, D. W., 1995: Warm rain process and WSR-88D. Western Region Tech. Attachment 95–08, 7 pp. [Available from NWS Western Region Headquarters, Federal Building, Salt Lake City, UT 84138.]
- Shafer, B. A., and M. Burke, 1979: SNOTEL. United States Geological Survey, U.S.G.S. Rep. 76-206, Reston, VA, 110–121. [Available from U.S. Geological Survey Library, 950 National Center, 12201 Sunrise Valley Dr., Reston, VA 20192.]
- Yang, D., B. E. Goodison, J. R. Metcalfe, V. S. Golubev, R. Bates, T. Pangburn, and C. L. Hanson, 1998: Accuracy of NWS 8” standard nonrecording precipitation gauge: Results and application of WMO intercomparison. *J. Atmos. Oceanic Technol.*, **15**, 54–68.

